sustainability

MDPI

Article

The Problem of Lighting in Underground Domes, Vaults, and Tunnel-Like Structures of Antiquity; An Application to the Sustainability of Prominent Asian Heritage (India, Korea, China)

Francisco Salguero Andujar [1], Inmaculada Rodriguez-Cunill [2] and Jose M. Cabeza-Lainez [2,*]

[1] School of Engineering, University of Huelva, Ctra, Huelva-Palos, 21071 Palos, Spain; salguero@didp.uhu.es
[2] School of Architecture, Architecture, University of Sevilla, 41012 Sevilla, Spain; cunill@us.es
* Correspondence: crowley@us.es; Tel.: +34-95-490-6793

Received: 30 September 2019; Accepted: 20 October 2019; Published: 22 October 2019

Abstract: Lighting in heritage is complex because of the forms intervening in it. The historical evolution of cultures has not been analytical and therefore, the shapes involved differ greatly from the cuboids typically found in 21st century architecture. As a vector, light inevitably attaches to surface sources. In this research, we focused on 3D curved geometries. Following a different trail to radiative transfer by virtue of detailed knowledge of the spatiality of volumes, we present new expressions, previously undefined in the literature, that are derived from a combination of surfaces that we have found in many archaeological sites around Asia. In the discussion, we start from the particularities of spherical surfaces where a normal vector has to pass through the center. By means of easy calculations, we deducted innovative laws. These in turn, allowed us to formulate several new expressions for configuration factors based on the adroit use of spherical fragments. The method easily extends to organic shapes that are often contained in the sustainable architecture of the past. The method finishes with suitable algorithms to assess the reflections in such curved forms. Finally, we implemented the results in our creative software. In this way, we enhanced the sustainable paradigms for heritage structures in Asia that we present as a conclusion of the article.

Keywords: lighting of tunnels and domes; Asian architecture; lighting of heritage; curvilinear radiative transfer; new solutions for equations of geometric optics

1. Introduction

The fundamental question of light in heritage architecture remains unsettled due to a lack of scientific advances in the field. The main objective of our research in this article was to implement the adroit correlations and expressions that we found, in order to deal with the variegated phenomena of light as it distributes over complex architectural surfaces from the past. It is known that daylight stems from surface sources. However, many designers do not properly understand the radiative performance of such surfaces, especially when typical cuboid shapes are absent, which is the main reason behind our efforts.

Disregard of surface sources of a three-dimensional shape in radiative transfer analysis is altogether usual. This can be explained by the complexities of the integral equations involved and is partly due to the want of a sufficiently geometric approach to the problem, if scholars come from fields of expertise outside design or architecture. When dealing with complex radiant surfaces, assimilation to a cluster of point sources is the base for the application of the iterative method common to finite element approaches in software, and sometimes direct integration is unable to yield adequate expressions, so only insufficient results exist for fewer basic forms [1,2]. By virtue of this, an ample list of meaningful

geometries that are often present in heritage architecture has remained neglected and energy waste or inaccuracies are evident. In order to increase the sustainability of the whole process from the restoration of ancient vestiges to public exhibition, we considered it necessary to start from a different approach.

In the ensuing research, we begin by focusing on the curved surfaces and derived shapes. Following a similar approach to radiation exchanges through detailed reflection on the particular details of different volumes, we hereby offer innovative and simpler expressions obtained from geometric adjustments that we have found in many sites around Asia.

As an initial discussion, we depart from the well-known spherical trigonometry. By means of basic calculation, we devised a new set of promising laws. These, in turn, result in previously unknown configuration factors for several fragments that involve the sphere. Afterward, the method can be extended to other organic shapes often contained in the architecture of the past.

In the second part, we accomplish the research by adding the equations concerned with finding inter-reflections in the said curved elements.

At all times, we conveyed the findings to an innovative software that enhances luminous radiative transfer simulation for a significant quantity of products and designs, especially of the paradigmatic cases that we give in our conclusions.

2. Physical Outline of the Problem

The reciprocity principle appears in Lambert's treatise *Photometria* [3], written in Latin in 1761 and is explicit in Equation (1). It produces the ensuing differential Equation (2), which still constitutes the scientific fundament of form factor exchanges for all kind of surfaces.

$$d\varnothing_{1-2} = (E_{b1} - E_{b2})cos\theta_1 \times cos\theta_2 x \frac{dA_1 x dA_2}{\pi x r^2} \quad (1)$$

$$\varnothing_{1-2} = (E_{b1} - E_{b2}) \int_{A_1} \int_{A_2} cos\theta_1 \times cos\theta_2 \times \frac{dA_1 x dA_2}{\pi x r^2} \quad (2)$$

where E_{bi} is the radiative power exiting from surface 1 or 2; A_i is the extension of each surface; dA_i is the elementary area; r is the vector that measures distance; and θ_i is the angle between distance vector and the normal to the surface for each elementary area considered (Figure 1).

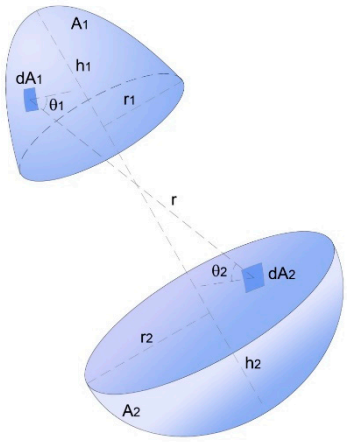

Figure 1. The reciprocity principle and equation for arbitrary surfaces A_1 and A_2.

The above equation indicates that radiative exchanges in any shape depend partly on the size, but also on its relative situation within the space under consideration (Figure 1). From the influential book of Lambert to the 21st century, engineers and scholars of either optics or radiation heat transfer have tried hard to find ways of solving the canonical Equation (2) for sundry elements [4]. This implies a

considerable effort as the said equation takes us on many occasion to a four-fold integration and the doubled primitive of simple functions implies many complex operations.

The variable, or internal part of the integral, is a dimensionless ratio called the form factor [1]. From the quantum electrodynamic point of view, the form factor represents the probability that the photons uniformly emitted from a certain surface can hit another to which it exposes in some manner [5]. Curvilinear forms may acquire distinct features that make a new system of calculation based on stable diffuse radiation, but without treating the integral directly, feasible [6].

3. Derivations from Spherical Caps

Beginning with elementary forms, it is possible to obtain a number of useful factors with perfect ease. It is only necessary to know the geometric properties of the intervening shapes. In a volume encircled by one surface, the sphere, let us consider diffuse irradiation to the inside of the form; in this case, the energy going to the interior of the volume has no way out and must be received on the same surface; if we call the spherical surface 1, the configuration factor to be found must be:

$$F_{11} = 1 \tag{3}$$

Considering the former for one-half of the sphere, the form factor could give $F_{11} = \frac{1}{2}$. In concordance with this familiar result, we decided to delve into the analysis of basic volumes composed of a limited number of surfaces. If we have two elements and one is flat (the base) and the other covers such a base in a sphere-like fashion, we would have a spherical cap.

Employing the previous finding to a spherical cap (called element 1), and the said disk of radius a (element 2); the radiative transfers in Figure 2 are deducted from the algebraic properties:

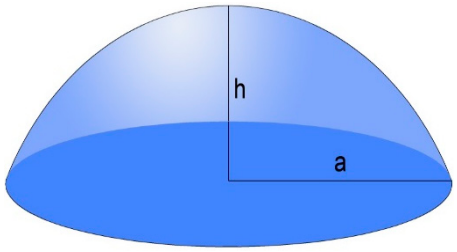

Figure 2. A spherical segment of uniform brightness featuring h as the height and radius a.

$A_1 x F_{12} = A_2 x F_{21}$. As $F_{21} = 1$, the expression produces $F_{12} = \frac{A_2}{A_1}$, and in this particular case:

$$F_{12} = \frac{a^2}{a^2 + h^2} \tag{4}$$

$$F_{11} = \frac{h^2}{a^2 + h^2} = \frac{h}{2 \times R} \tag{5}$$

Note that in planar surfaces F_{22} equals null.

A couple of basic principles are inferred from here. These are defined as the laws of Cabeza-Lainez.

The first principle says that:

For a volume composed of perfectly fitting elements presenting no internal obstruction and one of them being a disk, the view factor from the non-planar surface to the disk equates a fraction whose numerator is the area of the disk and the denominator is the area of the curved geometry.

The second principle of Cabeza-Lainez states that:

Under any spherical element, the so-called reflexive factor (or self-given energy) can be determined by the fraction of the area of the element divided by the total area of the spherical surface.

Bearing in mind that any segment of the sphere is the Nth fraction of the total surface (of radius R), and using Pythagoras's theorem,

$$(h^2 + a^2) = 2 \times R x h \tag{6}$$

Therefore,

$$N \times (h^2 + a^2) = 4 \times R^2 \; ; \; N = 2 \times \frac{R}{h} \; ; \; h = 2 \times \frac{R}{N} \tag{7}$$

This implies that

$$F_{11} = \frac{h}{2 \times R} = \frac{h^2 x N}{4 \times R^2} = \frac{1}{N} \tag{8}$$

The second principle informs us that the self-given energy for an Nth part of the sphere is a fraction of value 1/N. In this way, the previous supposition for one-half of the sphere is true; ensuing that divisions for one third or one quarter would give 1/3, 1/4, and so forth.

Such a principle will be fulfilled for many imaginable elements of the sphere that do not fall on typical categories as segments. Consequently, the properties expressed in Equations (5) and (8) are unique to the spherical surface and critical to settle the issue.

The former two principles can be extended to other adjustments that involve the sphere. Take for instance, a volume limited by two half-disks under any angle x, which varies between zero and π degrees (Figure 3):

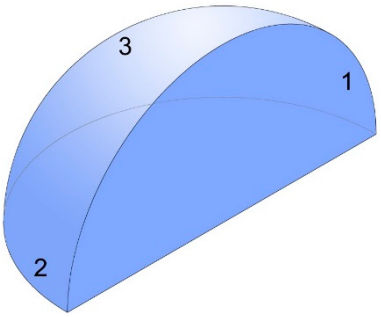

Figure 3. Depiction of elements in a spherical wedge, areas 1 and 2 show half-disks, and surface 3 is a part of the sphere.

Recalling the findings from above, the Nth fraction in the wedge gives $1/N = x/2\pi$ and so,

$$F_{33} = \frac{x}{2\pi} \tag{9}$$

Consequently,

$$F_{31} = F_{32} = \frac{1}{2} \times \left(1 - \frac{x}{2\pi}\right) \tag{10}$$

Incorporating the surfaces of the half-disks, $\pi R^2/2$

$$F_{13} = F_{23} = \frac{2x}{\pi} \times \left(1 - \frac{x}{2\pi}\right) \tag{11}$$

Continuing with the deduction at Equation (11), the pair of half-disks can cover any angle x ranging from 0 to π degrees (Figure 4). In this manner, the expression found below, and termed as the Cabeza-Lainez third law, is not described in any reference that we many know of [1]. Thus, we claim it to define the configuration factors that involve two semicircles with a common diameter, if x covers the magnitude of the angle comprised between them (Figure 5).

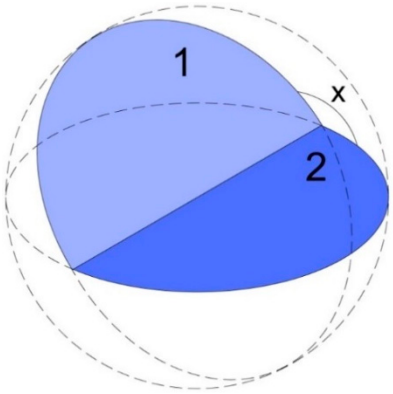

Figure 4. Two half-disks with equal radius R, sharing their diameters for any angle of X° degrees.

The above result simplified produces:

$$F_{12} = 1 - \frac{2\alpha}{\pi} + \left(\frac{\alpha}{\pi}\right)^2 \tag{12}$$

Transforming the equation into degrees,

$$F_{12} = 1 - \frac{x}{90} + \frac{x^2}{32400} \tag{13}$$

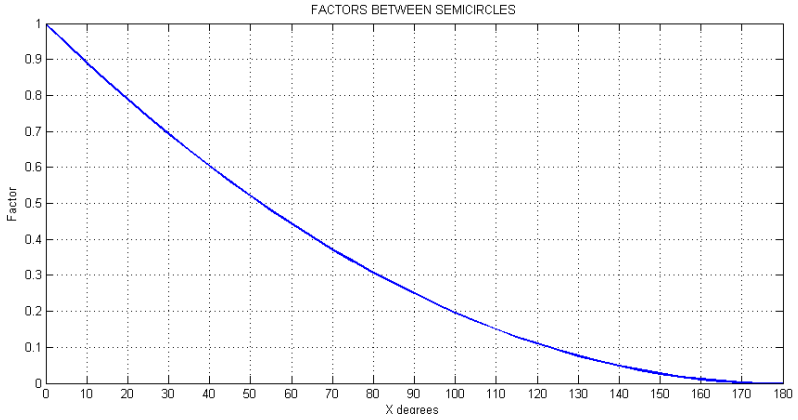

Figure 5. Luminous energy factors for two half-disks sharing the diameter and covering an angle of x^o sexagesimal degrees.

Cabeza-Lainez invented a fourth law based on the former (unpublished) and we can express it in the following way. For any couple of planar sections of a sphere (1–2) with a common edge and irrespective of the angle they form α, or if they pass through the center of the sphere or not, the form factor from surface 1 to surface 2 is:

$$F_{12} = \frac{A_1 + A_2 + A_3 \times (F_{33} - 1)}{2 \times A_1} = \frac{1}{2}\left(1 + \frac{A_2 - A_3}{A_1} + \frac{A_3^2}{A_s \times A_1}\right) \tag{14}$$

F_{33} is the factor of a sphere's fragment over itself, which is defined in the Cabeza-Lainez second law as the ratio between the area of the said fragment and the whole sphere (Equation (8)), in other words, $\frac{1}{2}$ for a hemisphere, $\frac{1}{4}$ for a quarter of sphere, and successively, it equals A_3/A_{sphere}.

A_i is the respective areas of surfaces 1 and 2 (segments of circle or ellipse), and 3 is the comprised fragment of the sphere (Figure 6).

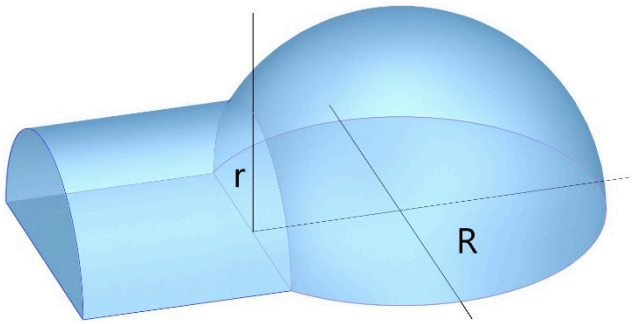

Figure 6. A spherical underground chamber susceptible to solve with our laws of radiation.

It is important to stress that Equations (12) to (14) have been demonstrated by numerical computation methods.

4. Further Developments

In Appendix A (Equations (A1) to (A12) and Figures A1–A3), a more complete collection of curved shapes to explain the different energy exchanges can be found. Following the discussion, we introduce an equation that correlates the radiative transfers of circular sectors with connected rectangles (Figure 7). This clearly applies to the geometry of the tunnel, a form that has been never been calculated previously due to is difficulty in integration [7].

For any vertical circular sector with a center situated in the middle of the edge x of a horizontal rectangle of dimensions x, y; by virtue of the Cabeza-Lainez seventh law, the form factor from the said rectangle to the sector of radius r will be (Figure 8):

$$\begin{gathered} t = r^2 + y^2 + x^2;\ m = \sqrt{x^2 \times \sin^2\theta_1 + y^2};\ n = \sqrt{x^2 \times \sin^2\theta_2 + y^2} \\ F_{21} = \frac{y}{2\pi} \times \left(\frac{cos\theta_1}{m} \times arctan \frac{r}{m + \frac{cos\theta_1 x}{m} \times (cos\theta_1 x - r)} - \frac{cos\theta_2}{n} \times arctan \frac{r}{n + \frac{cos\theta_2 x}{n} \times (cos\theta_2 x - r)} \right) \\ + \frac{y}{4\pi \times x} ln \left[\frac{(t - 2\ cos\theta_1 \times r \times x)}{(t - 2\ cos\theta_2 \times r \times x)} \right] \end{gathered} \tag{15}$$

The sector is comprised between the angles θ_2 and θ_1, being its radius r.

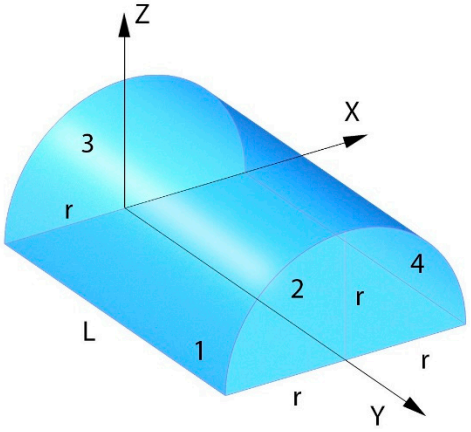

Figure 7. The surfaces and quantities that constitute a tunnel figure.

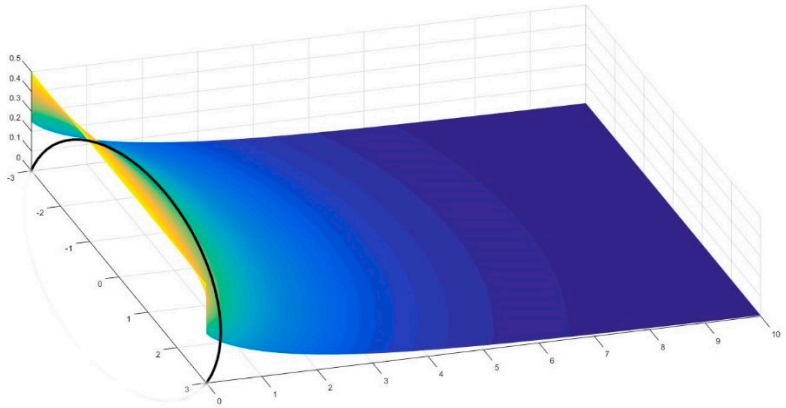

Figure 8. Energy distribution on the floor of a tunnel with a radius of 3 and a length of 10 (non-dimensional).

These important results lead to more possibilities of a simulation where different fragments of figures like conoids, spheres, cones, or circular sections are involved (Figure 8). All of these are very important to the appropriate study of lighting in heritage architecture, given that, as mentioned previously, the cuboid rarely appears in Asian or baroque temples [8].

Careful numerical integration methods give us the Cabeza-Lainez sixth law (Figure 9), which might be considered as a further generalization of the fourth law. We present them together in the graphs below (Figure 10).

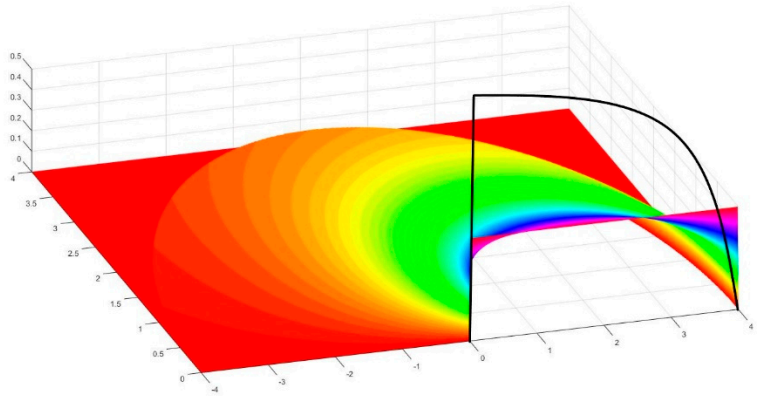

Figure 9. A quarter of a circle with a radius of 4 non-dimensional, and the energy spread over a semicircle with common edge.

The sixth law is described as:

$$F_{23} = 1 - 2 \times F_{21} - \frac{\alpha}{\pi} + \frac{1}{2}\left(\frac{\alpha}{\pi}\right)^2 \tag{16}$$

where α has the same angular meaning as before, but this time the law compares a quarter of the circles instead of semicircles.

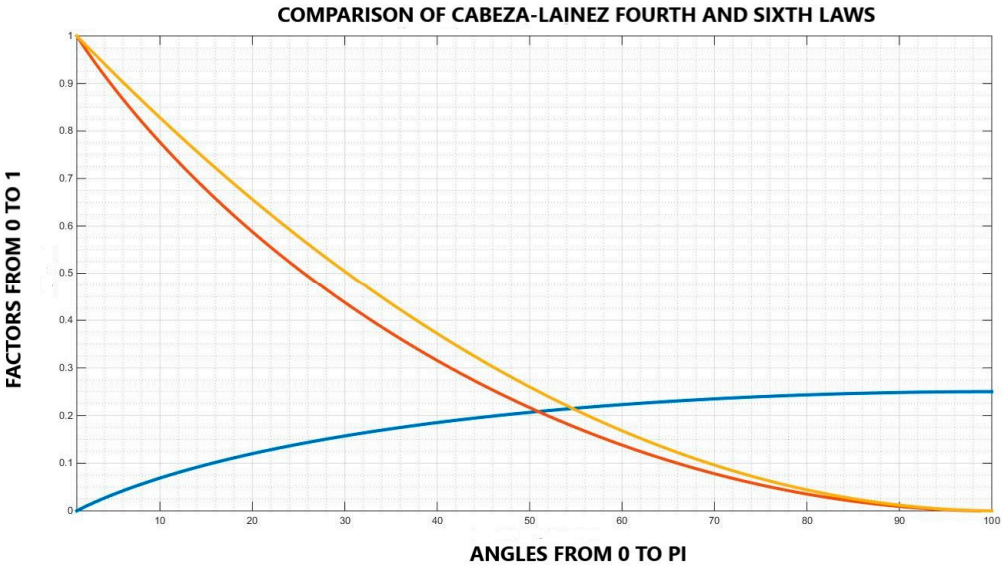

Figure 10. Fourth law (in orange) compared to the new sixth law (Equation (16), red), which directly connects to the seventh law (blue) f.

At this point of the discussion, we believe that a vast repertoire of unsuspected curved shapes in the literature has been covered in a robust way. Some other forms that have also been defined by the authors can be found in [9,10]. The forms solved can be applied with perfect ease to any kind of radiant energy, for example, artificial lighting, emitted heat, or daylight. In each case, we need to find the climatic data and boundary conditions that will appear in the particular problem considered. Appendix B (Equations (A13) and (A14)) gives some hints as to the above issue.

5. Inter-Reflections

One last point needs to be explained before presenting some relevant case studies, which is the question of inter-reflection. To this aim, we developed the following procedure.

The total balance of energy depends on the equation

$$E_{tot} = E_{dir} + E_{ref} \tag{17}$$

where E_{dir} is the fraction of direct energy and E_{ref} is the reflected fraction. If these quantities are summed, we obtain the global amount of radiation E_{tot}. Usually, several surfaces intervene in the process of reflection, and thus a set of expressions can be built. It is possible to introduce a pair of instrumental arrays that we will call F_d and F_r. For a volume enclosed by three surfaces (see Figure 11), such matrices would have the ensuing form:

$$F_d = \begin{pmatrix} F_{11} \times \rho_1 & F_{12} \times \rho_2 & F_{13} \times \rho_3 \\ F_{21} \times \rho_1 & F_{22} \times \rho_2 & F_{23} \times \rho_3 \\ F_{31} \times \rho_1 & F_{32} \times \rho_2 & F_{33} \times \rho_3 \end{pmatrix} \tag{18}$$

$$F_r = \begin{pmatrix} 1 & -F_{12} \times \rho_2 & -F_{13} \times \rho_3 \\ -F_{21} \times \rho_1 & 1 & -F_{23} \times \rho_3 \\ -F_{31} \times \rho_1 & -F_{32} \times \rho_2 & 1 \end{pmatrix} \tag{19}$$

with factors F_{ij} as previously found, yielding the energy transfer between the respective surfaces involved. Here, ρ_{i} represents the ratio of reflection (direct or otherwise) assigned to a particular element i [1].

Notice that in the matrix called F_d (Equation (18)) the diagonals are not null as the F_{ii} (with two ii) elements have definite values for curved surfaces, unlike the exchange in a cuboid.

If after careful integration by the procedures described previously, we are able to fix all the elements in Equations (18) and (19), we can establish new expressions (Equations (20)–(22)) in order to correlate the primary direct energy with the one extracted by reflections.

$$F_r \times E_{ref} = F_d \times E_{dir} \tag{20}$$

$$F_{rd} = F_r^{-1} \times F_d \tag{21}$$

$$E_{ref} = F_{rd} \times E_{dir} \tag{22}$$

As the amount of internally diffused energy is now a function of direct transfer, the problem is settled. A novel operation defined by Cabeza-Lainez is termed as the *product of form factors*, and being a sort of convolution operator it is still unrevealed how it applies in the calculation of these shapes.

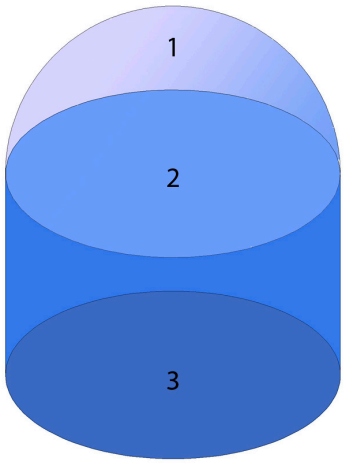

Figure 11. Volume composed only of curved figures, which is usual in heritage architecture.

6. Case Studies

6.1. Ajanta Caves and Underground Temples, India

For this article, we analyzed the Buddhist compound of Ajanta in the Wagora River, India, in detail. This consists of more than 30 artificial caves with either statues of the Buddha or frescoes of its past miraculous lives, also known as jataka [11,12]. The caves were excavated around the 5th century A.D. and could be clear precedents of the Silla Buddhist' temples of Korea (analyzed in Case Study 2).

In these famous underground temples, named Chaitya, daylight comes exclusively from an unglazed aperture, which resembles the semicircular mouth of a tunnel, although more prone to architectural expression. The reason behind these highly inspiring constructions is altogether sustainable (Figures 12 and 13).

When the Buddhist monks could not wander in pilgrimage preaching the doctrine of the dharma due to harsh monsoon weather, they instead decided to honor Shakyamuni by building stupas inside the cliff. In this manner, they protected themselves from discomfort, but still kept expounding the sutra, by virtue of prodigious images, to future believers.

The tunnel-like constructions were necessary to have some light and air during this hard but refined work, whilst the thermal inertia of the rock moderated the excessive oscillations in such a torrid region. Any waste material was accommodated in a natural fashion to the surroundings.

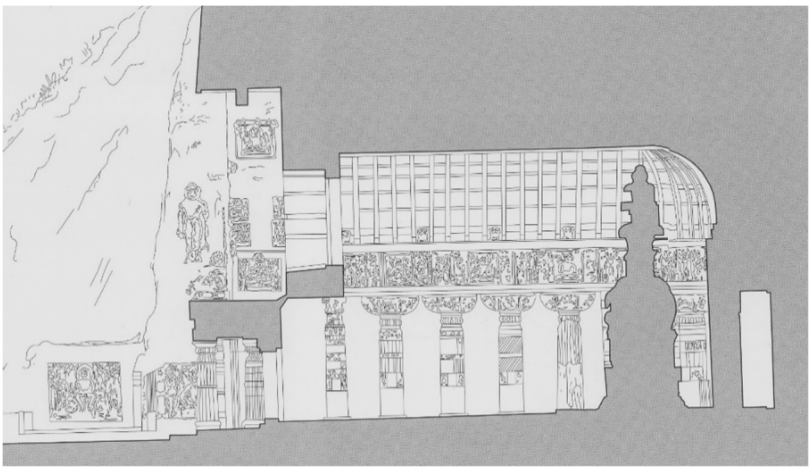

Figure 12. Section of Chaitya number 19.

Let us for instance describe the analysis performed in cave number 26 (Figure 14), which shows a western orientation that is ideal for ceremonies in early morning or evenings, depending on the season of the year.

(**a**) (**b**)

Figure 13. (**a**) View of the entrance to Chaitya number 26. (**b**) Interior stupa showing the sculpture of the Buddha.

By late summer, after the inevitable rainy season, the sky is cloudy (technically, overcast) and the illuminance levels may reach 10,000 lux. Assuming the radius of the opening to be 2 m and the span to the inner shrine is 14 m; we employed our tunnel shape simulation model to obtain, on the horizontal plane, values of only 6 lux. This means a very scant level of light (Figure 15).

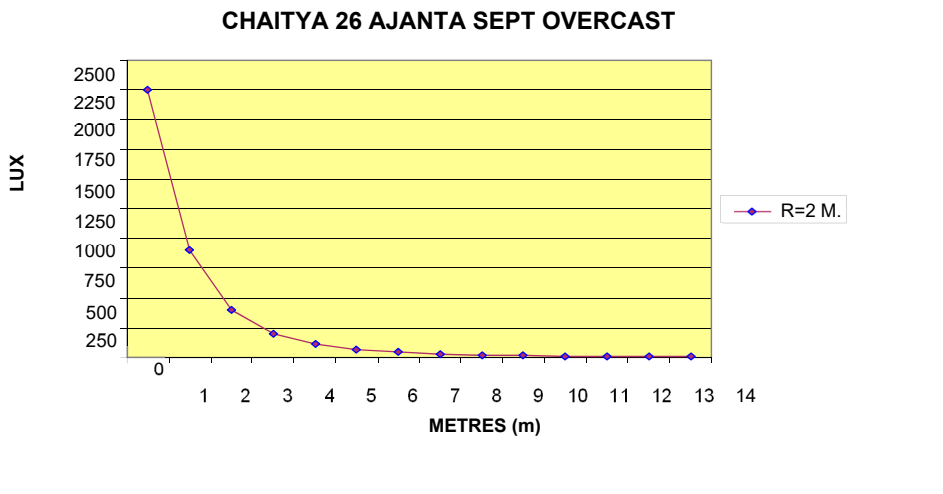

Figure 14. Graph of illuminance distribution in the chaitya. Source: Cabeza-Lainez.

Forewarned by this result, we suggested to the restoration team that inner reflections would be critical to perform any activities in the space, and that the materials employed should have enhanced extreme diffusion of light. Not much later, archaeological evidence corroborated this fact in remnants of stucco, gilt, or inlayed areas, and other kinds of reflective veneers.

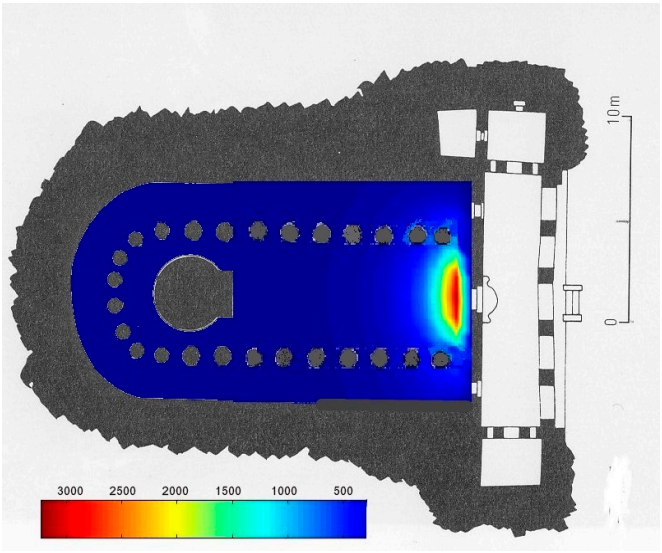

Figure 15. Plans of Chaitya 26 of Ajanta (India) with day-lighting values (3000–50 lux). Source: Cabeza-Lainez.

This was one of the first experiences with hypogeal precincts in Asia in which first-hand knowledge of sustainability through lighting was attained, but also in that it could help to raise meaningful restoration efforts.

6.2. The Seokguram Grotto, Gyeongju, Korea

Stimulated by our initial experience outside Europe, the Kyungil University invited us to research at another temple excavated in the mountain, which is in fact of paramount heritage for the Republic of Korea. It is also controversial from the point of view of political sustainability since it had been unearthed at the time of Japanese domain, and maintained for years in neglect and disrepair.

We had to carefully study the geometry and characteristics of the Seokguram Grotto (Figures 16–18), not only in connection with the sunlight, but also to determine the structural stability of the cupola enshrining the magnificent Buddha statue [13].

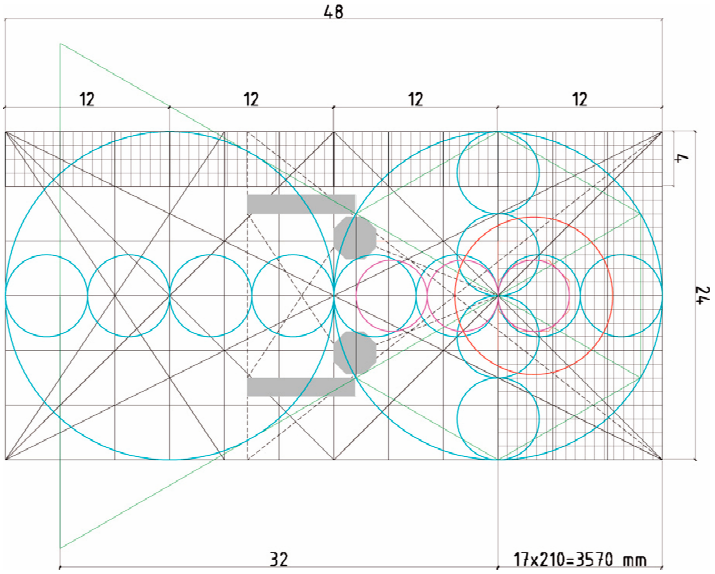

Figure 16. Geometric exactitude and proportions of the Seokguram artificial cave.

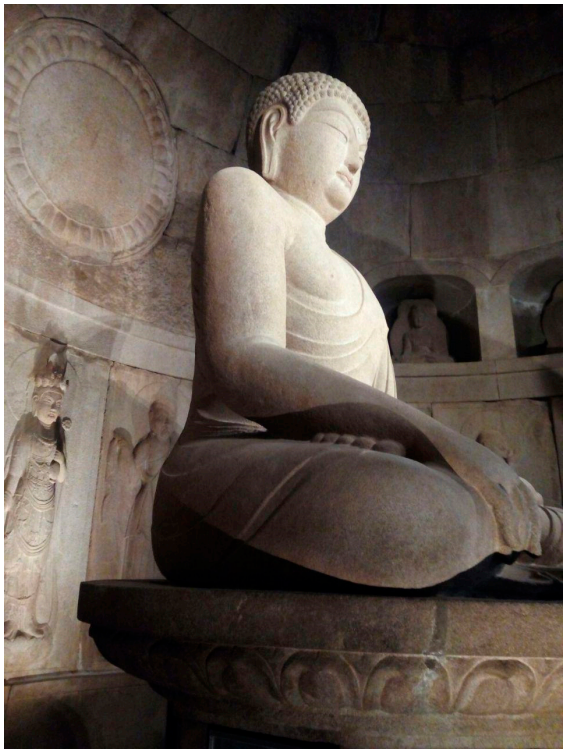

Figure 17. An interior view of the Buddha sculpture on a lotus pedestal. Source: Juhyung Lee.

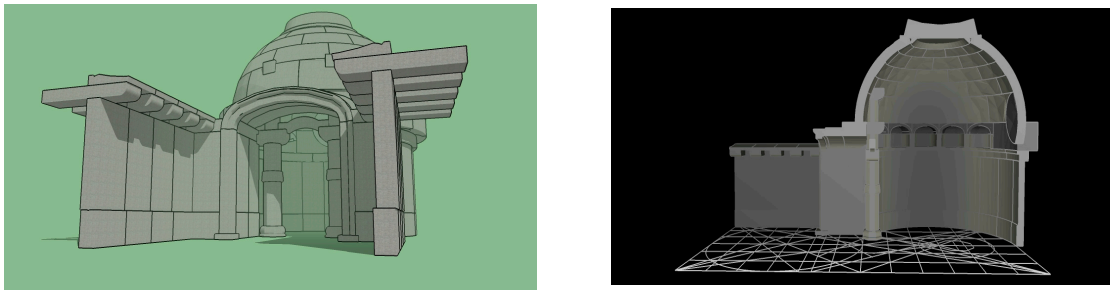

(**a**) (**b**)

Figure 18. Model of Seokguram underground temple. (**a**) View from the entrance of the model. (**b**) Interior with proportions and dome. Source: Salguero-Andujar.

We simulated the resistance and solidity of the new structure (Figure 19), which incorporated only fragments of the ancient one. The type of stone and the soil mechanics around the tumulus were also calculated [13].

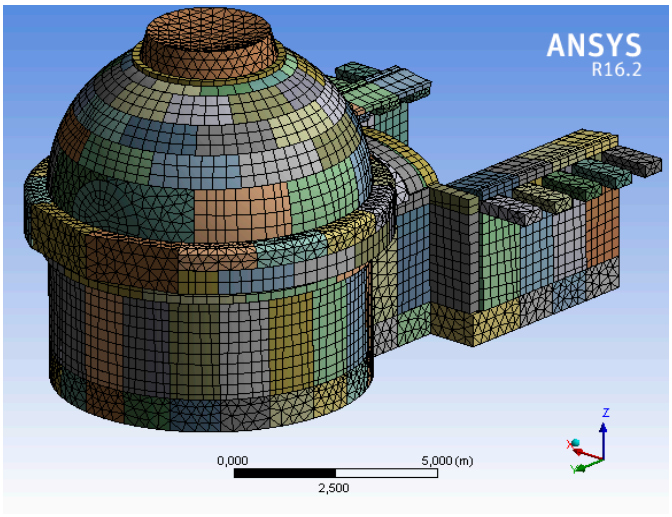

Figure 19. An example of the simulation model employed to find the stresses of the special type of granite stone employed for the dome. Source: Salguero-Andujar.

Finally, regarding the lighting conditions, we were asked to simulate the possibility of a circular opening with a diameter of 0.8 m in the low eastern area of the dome (Figure 20), which has been lost, according to evidence and other sources. Since this chamber is a spherical cap, the use of the equations presented in the previous chapters of the article was almost immediate and the results encouraging. However, we have to say that such a window would permit adumbrating the Statue of the Buddha, but common activities inside the temple would have to rely on reflections as in the case of Ajanta, or some sort of artificial lighting (Figure 21). We hope that in the near future and following our stint, some perforations of the dome could be implemented in accordance with a much more efficient electrical system.

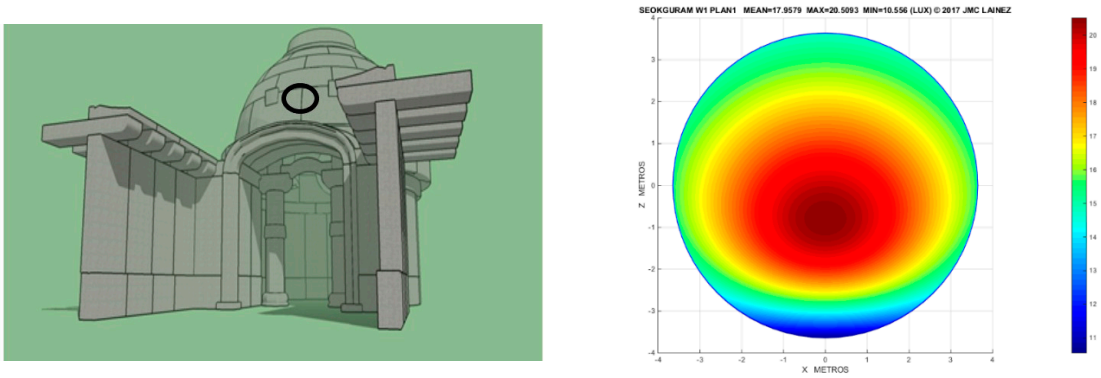

(**a**) (**b**)

Figure 20. Radiative model of Seokguram underground temple. (**a**) Tentative location of the archaeological opening (**b**) Distribution of daylight in the plan of the shrine, generated by the simulation software. Average values of 17.95 lux. Source: Cabeza-Lainez.

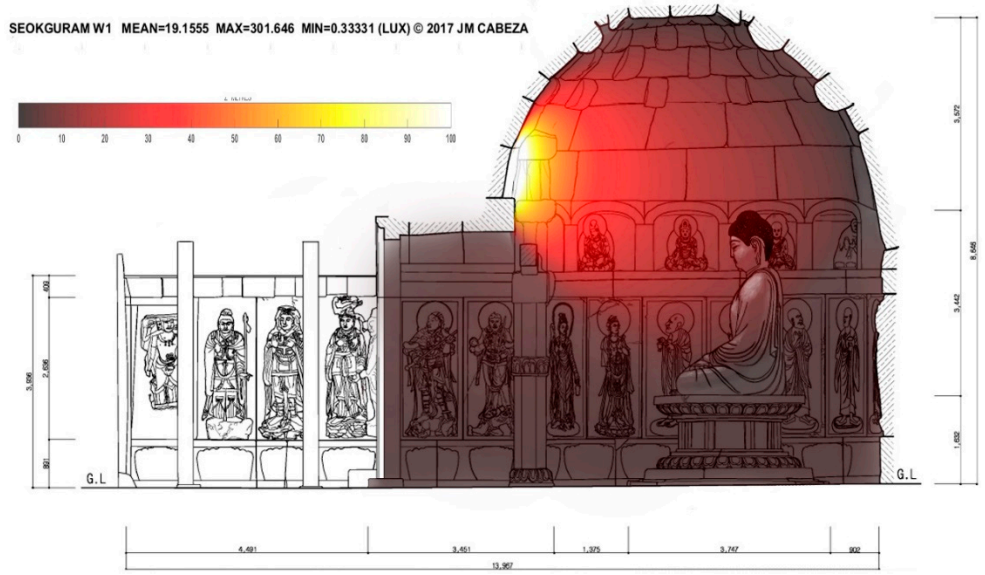

Figure 21. Sectional view of the grotto including lighting levels by a surmised circular opening. Source: Rodriguez-Cunill.

6.3. The Nantang Cathedral in Beijing, China

The third example discussed in this paper is no longer an extant catholic church in Beijing. It was built by Jesuit Missionaries at the beginning of the 17th century, but suffered several disasters until it was ruined by the second Opium War in the 19th century.

A new church was erected on the site, but it does not retain any of the excellent features that the former incorporated. The ancient church was a paradigm of Sinicization, as we will try to demonstrate (Figure 22).

The Jesuits had prepared detailed plans and a very unusual drawing perspective to facilitate the construction of the church.

Many curious features appear in the original drawings that the Portuguese Historic Archives maintain today. One of them is the triple ceremonial gate flanked by stone lions to protect the building from evil spirits.

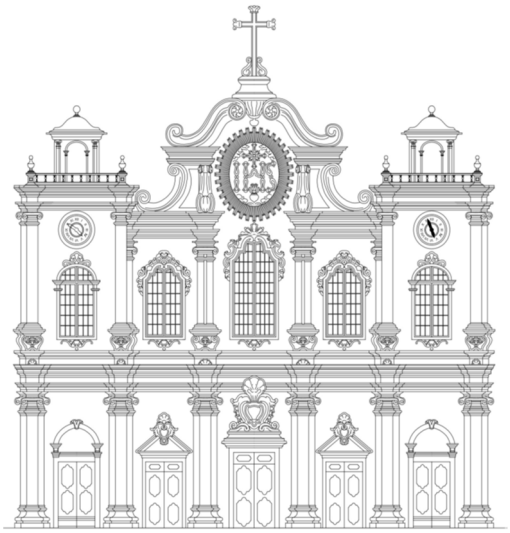

Figure 22. South façade of the Nantang Cathedral, reconstructed from the original plans preserved at the Arquivo Historico Ultramarino (Lisbon. Source: H. Ojeda and J. Cabeza-Lainez).

The plans present writings in Portuguese language, but detailed inscriptions in Chinese also appear. One such inscription shows the cardinal points or directions of Heaven, as mentioned in Daoist scriptures, specifically indicating that the main façade has to face due south for the same reason of harmonizing with the cosmos and to avert calamities [14].

Based on such magnificent drawings the authors have accurately reconstructed the floor plan and façade with the help of CAD systems.

The elevations reveal that the fundamental source of lighting was the main façade oriented to the south, which was in striking contrast with Catholic churches in Europe that usually face west, according to the authors' own surveys and measurements [8,15]. Here instead, slender framed windows are the sole elements of fenestration.

The overall style of the building did not resort to classic ornaments to resolve typical problems of expression, but rather seems to adopt baroque features as a starting point to create something new and capable of accommodating Chinese sensibility.

The Jesuits at the Qing Court had justly excelled in astronomical knowledge and subsequent control of time by manufacturing watches, astrolabes, and other mechanical tools of measurement for the Emperor. This fact is elegantly marked in the cathedral with the inclusion of two voluminous clocks at each side of the main façade, simultaneously displaying the time in Beijing and that of Rome.

The former indicates that they had guessed by exchanging letters in the occasion of eclipses, about the significant magnitude of the time lag between both places, although they were still unable to trace a meridian [15].

In this case, the simulation included the curved elements of the vaults that the European missionaries introduced as a novelty for interior spaces. The vault and the dome had not developed much in Eastern Asia for several reasons including the want of compressive materials and weather tending to heavy rains and winds [14].

In Figure 23, we present the trajectories of solar movement for the vicinity of the church and its probable exposure to sunlight.

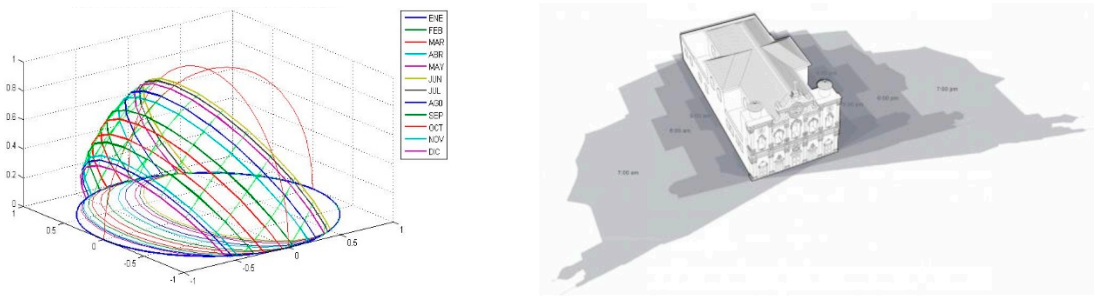

(**a**) (**b**)

Figure 23. Daylighting model of Nantang Cathedral. (**a**) Solar Chart for Beijing. (**b**) Solar exposure at different hours. Source: Cabeza-Lainez.

Figures 24 and 25 depict a more vectorial approach to the radiation phenomena of the interior for the situations of summer and winter.

As previously stated, the key here is the southern orientation of the main façade, which is very unusual in the West, but required from cosmological and cultural points of view. Such disposition may have contradicted the catholic liturgy on many occasions.

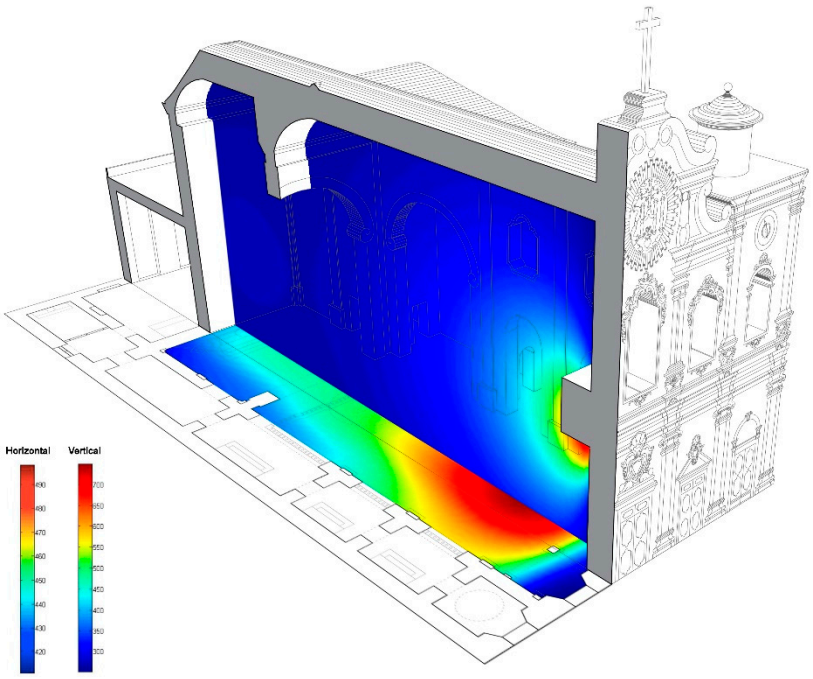

Figure 24. Radiative field inside the church in winter. Source Cabeza-Lainez.

The levels were revealed to be adequate for the performance of activities in the range of 400 lux. This is important because most Chinese temples and precincts were dark and gloomy and a new religion could easily prove its supremacy by revealing even the darkest corners of its faith by means of its architecture.

If harmony with thesun and environment is demonstrated by virtue of architecture, it is easier to spread any belief that is taught precisely at that architecture. The Jesuits were always conscious of such a fact in all of their churches [16].

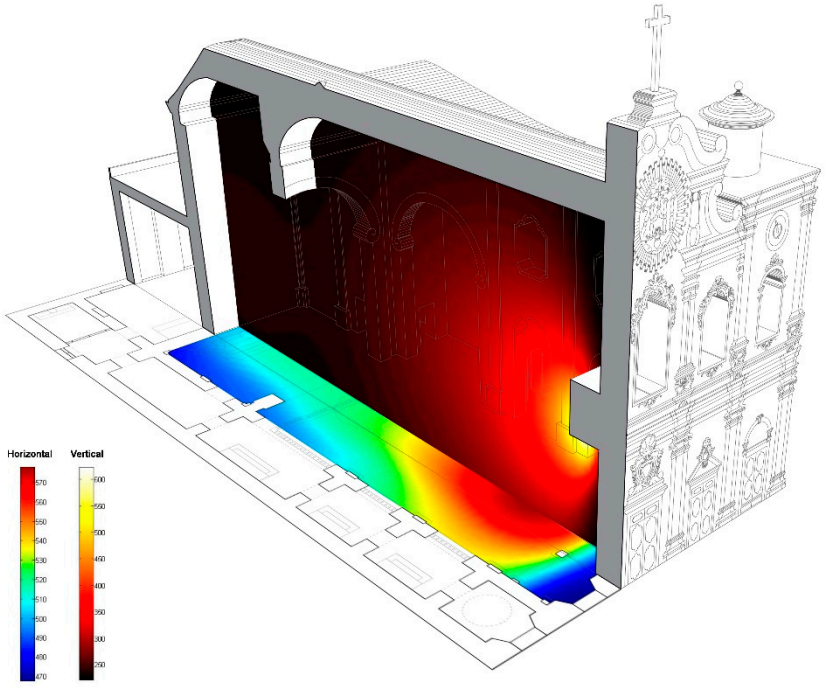

Figure 25. Summer distribution of radiation for the Nantang Cathedral. Source: Cabeza-Lainez.

Except for the façade, the exterior of the church remains simple in character. However, from another original etching, we know that the interior was lavishly decorated, the ceilings were vaulted with carved and painted wooden panels using naturalistic motifs. It is on the inner walls of the Cathedral that the spectacular frescoes of Giuseppe Castiglione once stood.

Master Castiglione, or Lang Shining in Chinese, was considered by many to be the last great Chinese painter who used another European effect to beckon the believers: focal perspective. As a curiosity, we reconstructed the following descriptions of the contemporaries of some of the paintings that once adorned the interiors conceived by Castiglione. We can only regret that they are lost . . . forever? (Figure 26).

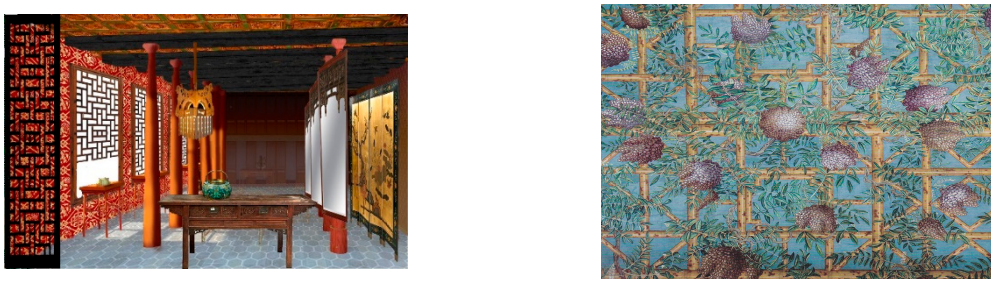

(**a**) (**b**)

Figure 26. Frescoes by Giuseppe Castiglione. (**a**) Reconstruction of Nantang Cathedral. (**b**) Inside the JuanqinZhai (Pavillion at the Forbidden City) pergola of wisteria. Source: Rodriguez-Cunill.

7. Discussion

Through the previous paragraphs, we have readily made available an ample scope of possibilities for sustainable lighting in the heritage of East Asia. New principles proposed by the authors have been devised and incorporated to facilitate the simulation process of many curvilinear geometries. Such innovative formulations are difficult to obtain, but still, due to their mathematical exactitude, the radiative transfer procedures are significantly clarified and valuable computational time is reduced to

a mere fraction in comparison with previous analysis. The complex issue of inter-reflections in curved volumes has been completed with perfect ease and this is an important novelty.

Regarding the monuments presented as case studies, some of them have been rebuilt (Seokguram) and the Nantang Cathedral is no longer extant. Therefore, we cannot monitor them properly to check the hypothesis is validated. We have to trust in other studies that the authors conducted in European heritage. For example, the Guarini Church in Torino (Italy), the Jesuit novitiate of San Luis (Seville), or the research initiated at the Egyptian Hall of Thutmose III in Luxor. We feel that perhaps more detailed work should still be done on the less complex aspect of the issue: the artificial lighting of such precincts. However, this is resolved in most cases by national consultants with little or no intervention of foreign experts and techniques. We would like to stress that all the methods hereby presented are suitable for immediate application to every kind of fixture or luminaire, and is especially appropriate for Light Emitting Diodes (LED systems, which tend to become surface distributed sources of low intensity and energy consumption.

Our unceasing effort to bring light to the darkest depths appears to be similar to the myth exposed in the Platonic cave. Nonetheless, we still believe that lighting design and predictions are a valuable resort for the qualification of the space and of heritage in this fashion. We only strive to provide a foremost advance in the scientific knowledge of design sources for natural light and issue clear expedients of how the prediction of the dynamic (radiant) energy and climate response of very resilient architectural structures has produced real sustainability through the ages.

The findings hereby reveal, for instance, to what extreme cross-cultural relationships influenced the development of the so-called Baroque Reason, which extends from Mathematics and Geometry to Art and Design. Adopting the architectural point of view, the lessons that we are to learn relate with adequacy to the climate and harmonious sustainable coexistence between the environment and civilization. A superb weapon for the fight against climate change.

Not in vain, the Swiss architectural historian, Sigfried Giedion once stated: "it is light that induces the sensation of space. Space is annihilated by darkness. If light is eliminated, the emotional content of space disappears, becomes impossible to apprehend. In the dark there is no difference between the emotional evaluation of a chasm and of a highly modeled interior." [17], p. 495.

Decades have passed since this wise dictum was pronounced and yet architecture, in a word, does not seem fit to sustain life on our menaced planet.

A sad paradox, as it is clear that if we can neither separate history from climate nor climate from history, then, how are we to live?

The Chinese sage Zhuangzi suggested, "Be Infinite like space and the four directions—they are boundless and form no enclosures. Sustain all things in your love."

Author Contributions: I.R.-C. and J.M.C.-L. were helpful in conceptualizing the scope and issues. F.S.A. brought the instrumentation and the structural software as well as the momentum at low tide epochs. J.M.C.-L. developed the software for radiative simulation and created algorithms that sustained the whole process. I.R.-C. was instrumental in visualizing the cultural and artistic implications of our work.

Funding: This research received no external funding.

Acknowledgments: Francisco Salguero Andujar appreciates the kindness and help of Juhyung Lee and all the personnel at Seokguram. Inmaculada Rodriguez Cunill desires to honor the memory of Antonia Cunill Aragon by virtue of her contribution. Ioseph Cabeza-Lainez would like to dedicate this article to Jose Cuadrado Moreno for his continuous support and endurance. Ana, Rocio, and Humphrey Ojeda are well remembered.

Conflicts of Interest: The authors declare no conflict of interest.

Appendix A

In the discussion that we sustained at point 3 about the spherical cap; we demonstrated that the necessary form factor was (Equation (4)),

$$F_{12} = \frac{a^2}{a^2 + h^2}\,. \tag{A1}$$

If we may define a fraction β, composed of the squared heights and radiuses, expression A1 is reduced as

$$\beta = \frac{h^2}{a^2} \tag{A2}$$

$$F_{12} = \frac{1}{\beta^2 + 1} \tag{A3}$$

- Since the Cabeza-Lainez first law is more encompassing, it can be used for other curved elements outside of the sphere, like the conoid and the hyperboloid.
- Prolate Semispheroid (Figure A1)

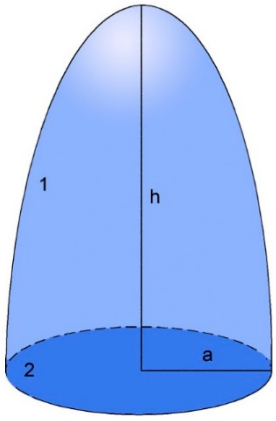

Figure A1. Prolate spheroid.

Element 1 is an oblong ellipsoid and element 2 is the circle that serves as a base to the curved figure, h > a.

Previously, we defined the dimensionless relation m:

$$m = \sqrt{1 - \frac{a^2}{h^2}} \tag{A4}$$

Employing the first law,

$$F_{12} = \frac{a \times m}{a \times m + h \times \arcsin(m)} \tag{A5}$$

$$F_{21} = 1 \tag{A6}$$

$$F_{11} = \frac{h \times \arcsin(m)}{a \times m + h \times \arcsin(m)} \tag{A7}$$

Making it as before in the spherical cap

$$\beta = \frac{h^2}{a^2};\ m = \sqrt{1 - \frac{1}{\beta^2}} \tag{A8}$$

$$F_{12} = \frac{\sqrt{1 - \frac{1}{\beta^2}}}{\sqrt{1 - \frac{1}{\beta^2}} + \beta \times \arcsin\left(\sqrt{1 - \frac{1}{\beta^2}}\right)} \tag{A9}$$

- Paraboloid of revolution (Figure A2).

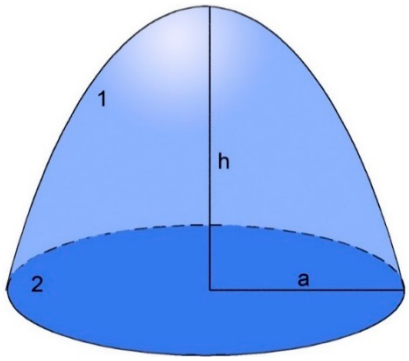

Figure A2. Paraboloid of revolution.

In this case, element 1 is the paraboloid and element 2 is the circle that serves as a base to the upper curved surface

$$F_{12} = \frac{6 \times a \times h^2}{\left[\left(a^2 + 4 \times h^2\right)^{3/2} - a^3\right]} \times F_{21} = 1 \tag{A10}$$

$$F_{11} = 1 - \frac{6 \times a \times h^2}{\left[\left(a^2 + 4 \times h^2\right)^{3/2} - a^3\right]} \tag{A11}$$

$$\beta = \frac{h}{a} \times F_{12} = \frac{6 \times \beta^2}{\left[\left(1 + 4 \times \beta^2\right)^{3/2} - 1\right]} \tag{A12}$$

In Figure A3, we plotted the evolution of factor F_{12} for some usual geometric bodies. The cone presents higher values of emitted energy while the sphere and the ellipsoid are less prone to diffuse radiation internally. Other forms such as the conoid or the hyperboloid could be included in the future.

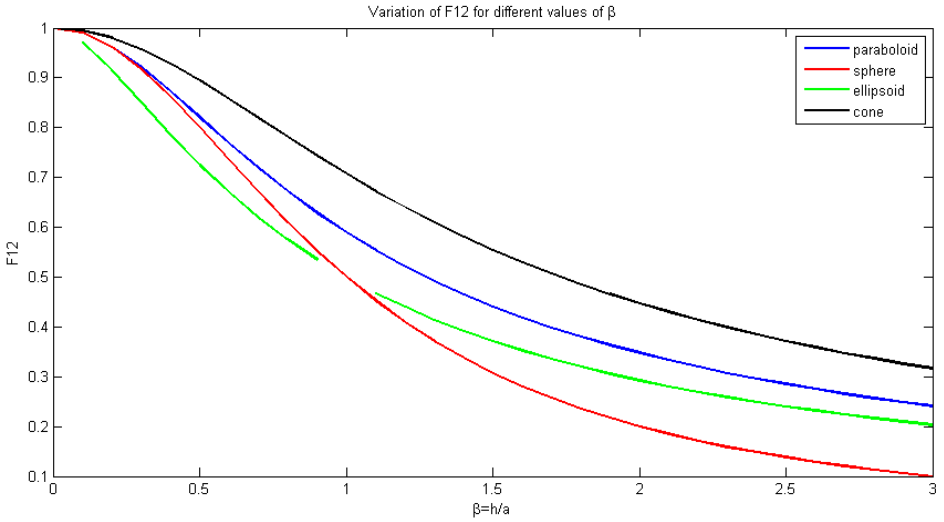

Figure A3. Comparison of four common curved geometries (non-dimensional).

Appendix B

Some useful formulas proposed in the absence of direct climatic data of irradiance.

To study the incidence of radiation on a vertical surface, we need to resort to formulas somewhat more complex. For the clear sky, vertical illuminance due to a half-hemisphere is, following Gillete and Pierpoint [18],

$$E_v = 4000 \times \theta^{1.3} + 12000 \times \sin^{0.3} \theta x \cos^{1.3} \theta \times \left[\frac{2 + \cos \varnothing}{3 - \cos \varnothing}\right], \tag{A13}$$

where $\emptyset$ is the azimuth, and θ is the solar altitude.

The algorithm allows the daylight intensities to be obtained for the vertical and horizontal surfaces as a function of the location's latitude. In the situation of an overcast sky, typically defined by the CIE standards, the former expression simplifies as:

$$E_v = 8500\ \mathrm{xsin}\theta, \tag{A14}$$

The authors have also proposed a computer simulation program (not detailed here) that automatically gives the data required, following a few input parameters like solar altitude, the number of sun-hours per month, and the cloudiness index, if available.

References

1. Cabeza-Lainez, J.M. *Fundamentals of Luminous Radiative Transfer*; Netbiblo: Seville, Spain, 2010. (In Spanish)
2. Moon, P.H.; Spencer, D.E. *The Photic Field*; The MIT Press: Cambridge, MA, USA, 1981.
3. Lambert, J.H. *Photometry, or, on the Measure and Gradations of Light, Colors and Shade*; DiLaura, D.L., Ed.; Illuminating Engineering Society of North America: New York, NY, USA, 2001.
4. Higbie, H. *Lighting Calculations*; JohnWiley & Sons: New York, NY, USA, 1934.
5. Feynman, R. *Quantum Electrodynamics: The Strange Theory of Light and Matter*; Penguin Books: London, UK, 1990.
6. Yamauchi, J. Theory of Field of Illumination. *Res. Electro Tech. Labor.* **1932**, *339*, 1–37.
7. Yamauchi, J. The Light Flux Distribution of a System of Interreflecting Surfaces. *Res. Electro Tech. Labor.* **1927**, *190*, 1–91.
8. Almodovar-Melendo, J.M.; Cabeza-Lainez, J.M.; Rodríguez-Cunill, I. Lighting Features in Historical Buildings: Scientific Analysis of the Church of Saint Louis of the Frenchmen in Seville. *Sustainability* **2018**, *10*, 3552. [CrossRef]
9. Howell, J.R. *A Catalog of Radiation Configuration Factors*; University of Texas: Austin, TX, USA, 1982; ISBN 978-0-07-030606-6. Online version (2019); Available online: http://www.thermalradiation.net/indexCat.html (accessed on 18 September 2019).
10. Modest, M.F. *Radiative Heat Transfer*, 3rd ed.; Academic Press Elsevier: San Francisco, CA, USA, 2013.
11. Jain, K.; Jain, M. *Thematic Space in Indian Architecture*; India Research Press: New Delhi, India, 2002.
12. Kamiya, T. *The Guide to the Architecture of the Indian Subcontinent*; Toto Shuppansha: Tokyo, Japan, 1996.
13. Salguero Andujar, F. Comparative, geometric and structural analysis of the Seokguram Temple at Gyeongju (Korea). In Proceedings of the International Conference on Advances on Heritage Preservation, Korea, Gyeongju, September 2017; pp. 3–1031.
14. Cabeza-Lainez, J.M.; Almodóvar-Melendo, J.M. Daylight, Shape, and Cross-Cultural Influences Through the Routes of Discoveries: The Case of Baroque Temples. *Space Cult.* **2018**, *21*, 340–357. [CrossRef]
15. Almodovar-Melendo, J.M.; Cabeza-Lainez, J.M. Environmental Features of Chinese Architectural Heritage: The Standardization of Form in the Pursuit of Equilibrium with Nature. *Sustainability* **2018**, *10*, 2443. [CrossRef]
16. Rodríguez-Cunill, I. Pintar a través del ojo de la cámara. *Rev. Int. Comun. Audiov. Public. Lit.* **2004**, *1*, 51–65.
17. Giedion, S. *The Eternal Present. The Beginnings of Architecture*; Bollingen Foundation: Princeton, NJ, USA, 1964; p. 495.
18. Pierpoint, W. A Simple Sky Model for Daylighting Calculations. In Proceedings of the International Daylighting Conference, Phoenix, AZ, USA, 16–18 February 1983.